

MIXTURE MODELS FOR STUDYING STELLAR POPULATIONS: BIVARIATE RELATIONSHIPS AND POSTERIOR MIXING PROPORTIONS APPLICABLE TO THE THICK-DISK PROBLEM

JAMES M. NEMEC
Program in Astronomy
Washington State University
Pullman, WA 99164-3112 USA

AMANDA F. LINNELL NEMEC
International Statistics and Research Corp.
P.O. Box 496, Brentwood Bay
British Columbia, V0S 1A0 Canada

ABSTRACT. Finite mixture models provide a useful framework for analysing the overlapping spatial, kinematical, chemical, and age distributions of stellar populations. In this paper, the age-metallicity relationship is used to illustrate the properties of bivariate mixture distributions. The interpretation of bivariate scatter plots and ‘binning’ diagrams is discussed, and population membership is examined by computing posterior mixing proportions.

1. Introduction

It is generally recognized that in the solar neighbourhood there exist stars of all ages, up to $A \sim 15$ Gyr. These stars are known to exhibit a diversity of chemical compositions, ranging from $[\text{Fe}/\text{H}] \sim 0.3$ to -4.0 dex, and have space motions corresponding to U velocities (directed away from the Galactic center) and W velocities (directed toward the North Galactic Pole) between -200 and $+200 \text{ km s}^{-1}$, and V velocities (in the direction of Galactic rotation) between -400 and $+50 \text{ km s}^{-1}$. The observed *overall* distribution functions of the variables U and W are symmetric about zero (*i.e.*, the motions are symmetric about the local standard of rest). In contrast, the overall distribution functions for A , $[\text{Fe}/\text{H}]$, and V are asymmetric. The asymmetry in the V distribution is the well-known asymmetric drift.

The notion that stars in the solar neighbourhood constitute a mixture of discrete stellar populations can be traced to the early ideas on stellar kinematics of Kapteyn, Schwarzschild, and Eddington. The modern concept of a stellar population originated with Baade’s 1944 introduction of Populations I and II for modelling galaxies, and the five-component model for the Galaxy advocated at the 1957 Vatican conference. Within the last ten years, there has been considerable discussion about the number of distinct components that are needed to represent the chemical and dynamical history of our Galaxy (see Sandage 1987b), the proportion of stars belonging to each component, and the nature of the individual components. Much of this debate has been fuelled by various theories for the early evolutionary phases of our Galaxy (Eggen, Lynden-Bell & Sandage 1962, Searle and Zinn 1978, Norris & Ryan 1989).

According to the Bahcall & Soneira model (see Bahcall 1986), the solar neighbourhood can be represented by only two stellar populations - a disk (D) and a halo (H) - with 99.8% of the nearby stars brighter than $M_V = 16.5$ belonging to the disk component, and only 0.2% belonging

to the halo, *i.e.*, D:H=500:1. Owing to uncertainty in the estimated mixing proportions, the ratio might actually be $\sim 2\text{--}4$ times greater than the quoted value. The Norris & Ryan model is another example of a two-component model, but in that case the two components comprise an extended disk component and a discrete halo. In contrast, proponents of the Gilmore-Reid-Wyse three-component model claim that the Galaxy has three distinct components - a flat thin disk (t), a spheroidal halo (h), and an intermediate thick disk (T). Estimated mixing proportions for this model range from a t:T:h ratio of 200:22:1 (Sandage 1987a) to a ratio of 1200:20:1 (Gilmore & Wyse 1985).

The ratios quoted above are estimates of the *true* or *absolute* mixing proportions of the components that make up the two- or three-component model. These ratios are obviously of interest since they have a direct bearing on questions related to the vertical acceleration, K_z , and dark matter in the solar neighbourhood. However, because complete samples are rarely available in practice, it is generally difficult to determine the true mixing proportions. For most samples, only the *apparent* mixing proportions (which depend on the survey limits, the location of the survey volume, and other imposed selection criteria) can be estimated directly.

Determination of the appropriate number of components and estimation of either the true or apparent mixing proportions are two essential steps in modelling galactic structure. The nature of the individual components is also an important consideration. This aspect of the model has raised questions about the shapes of the underlying within-component distribution functions, in particular whether there are correlations between age, kinematical and chemical variables, *e.g.*, metallicity and other gradients within the components. These questions must be answered if the 'best' fitting model is to be identified.

For simplicity, the discussion in this paper is limited to bivariate mixture models. After briefly reviewing the fundamental ideas on which finite mixture models are based (§2), we discuss bivariate scatter plots and 'binning' diagrams (§3), and bivariate posterior mixing proportions (§4). Such topics as parameter estimation, and the problem of the optimum number of components, were discussed in Nemeč & Nemeč (1991a, hereafter Paper I), and in Nemeč & Nemeč (1991b, hereafter Paper II), and will not be repeated here. Generalization of the bivariate mixture model to the multivariate case is straightforward. The reader is referred to Papers I and II, and the references therein, for a more detailed exposition of univariate and multivariate mixture models and their application to the study of stellar populations.

2. Bivariate Mixture Model for Age-[Fe/H] Relationship

To illustrate the application of mixture models to stellar population problems (in particular the thick-disk problem), we consider here an idealized age-metallicity relationship for the solar neighbourhood (*i.e.*, stars with distances nearer than about 500 pc), which will be assumed to comprise thin-disk, thick-disk, and halo stars. The basic equation for a three-component mixture model is

$$f(A, m) = \sum_{k=1}^3 p_k f(A, m|k), \quad (1)$$

where $f(A, m)$ is the overall *joint* or *bivariate* probability density function of age (A) and metallicity ($m = [\text{Fe}/\text{H}]$), p_k is the mixing proportion for the k^{th} population, and $f(A, m|k)$ is the corresponding joint density function of the k^{th} component ($k = 1, 2, 3$). To obtain the univariate, or *marginal*, density function of an individual variable (in this case, A or m), the joint density function (Eqn. 1) is integrated over the other variable. The result is a univariate mixture distribution with the same mixing proportions as the joint distribution.

According to Eqn. 1, if the true mixing proportions are in the ratio t:T:h=200:20:1 (see above), then one would expect to find, in a random sample of 1000 nearby stars, ~ 905 thin-disk

stars, ~ 90 thick-disk stars, and ~ 5 halo stars, each of which would have an age and a metallicity drawn from their respective within-component joint distribution functions of A and $[\text{Fe}/\text{H}]$, *i.e.*, $f(A, m|k)$. For a sample of stars selected in a way that strongly favours nearby halo and thick-disk stars (e.g., the Sandage & Fouts 1987a and Carney *et al.* 1989 samples, which consist of high-proper-motion stars drawn from the Lowell proper motion survey), the true mixing proportions are replaced by sample-dependent apparent mixing proportions, *e.g.*, t:T:h=2:2:1.

At present, the forms of the within-component distribution functions are not well known. However, there is little evidence to suggest that a bivariate Gaussian distribution is not a good first order approximation. We will, therefore, assume that the within-component distributions are Gaussian. Thus,

$$f(A, m|k) = [2\pi\sigma_{mk}\sigma_{Ak}(1 - \rho_k^2)^{1/2}]^{-1} \exp\{-Q_k\} \quad (2)$$

where

$$Q_k = \frac{1}{2(1 - \rho_k^2)} \left[\frac{(m - \mu_{mk})^2}{\sigma_{mk}^2} + \frac{(A - \mu_{Ak})^2}{\sigma_{Ak}^2} - 2\rho_k \frac{(m - \mu_{mk})(A - \mu_{Ak})}{\sigma_{mk}\sigma_{Ak}} \right],$$

and

$$\rho_k = \frac{\text{Cov}_k(A, m)}{\sigma_{Ak}\sigma_{mk}}$$

is the (Pearson) correlation between m and A for component k .

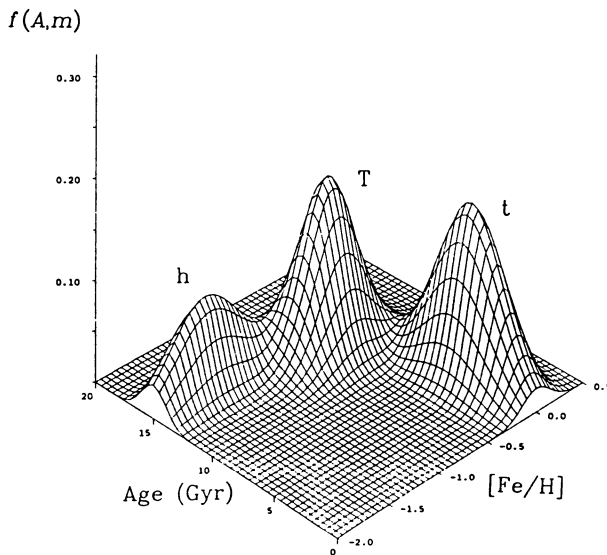


Figure 1. Overall bivariate distribution function corresponding to the A - $[\text{Fe}/\text{H}]$ relationship for solar neighborhood stars.

Fig.1 illustrates a typical overall age-metallicity distribution that might arise under a Gaussian mixture model. The plot was generated by substituting a particular set of parameter values into Eqn. 2 and plotting the resultant mixture density function. For the (apparent)

mixing proportions, we have substituted 20% halo, 40% thick disk, and 40% thin disk, which are consistent with the values that might be expected for high-proper-motion samples of the type mentioned above. For the means and standard deviations of the three components, we have adopted the following parameters: for the halo, a mean metallicity of $\mu_{mh} = -1.50$ dex, with a standard deviation of $\sigma_{mh} = 0.35$ dex, and a mean age of $\mu_{Ah} = 15$ Gyr, with a standard deviation of $\sigma_{Ah} = 1$ Gyr; for the thick disk, a mean metallicity $\mu_{mT} = -0.50$ dex, with a standard deviation of $\sigma_{mT} = 0.25$ dex, and a mean age of $\mu_{AT} = 13$ Gyr, with a standard deviation of $\sigma_{AT} = 1.5$ Gyr; and for the thin disk, a mean metallicity of $\mu_{mt} = 0$ dex, with a standard deviation of $\sigma_{mt} = 0.15$ dex, and a mean age of $\mu_{At} = 5$ Gyr, with a standard deviation of $\sigma_{At} = 2.5$ Gyr. These values were chosen to be representative of recent estimates (see Paper I). We have also assumed that m and A are statistically independent for each component, *i.e.*, $\rho_k = 0$ for $k = 1, 2, 3$.

The number of distinct peaks in Fig. 1 is clearly equal to three. However, because the means for the individual components may be less well separated for some pairs of variables, the thick-disk might be less obvious in such bivariate plots as the Bottlinger U - V diagram, the V - m diagram, and the W - m diagram (see Nemeč & Nemeč 1992, in preparation). Of course, if these bivariate plots are compared with plots of the corresponding marginal distributions (cf. Fig. 1 of this paper and Fig. 1 of Paper I), it is evident that the ability to discriminate components improves as additional variables are taken into consideration.

In Fig. 1, we assumed that A and m are independently distributed for each component k , *i.e.*, there are no *within-component gradients*. To test the validity of this assumption, it is sufficient, in the Gaussian case, to test the null hypothesis that $\rho_k = 0$ for $k = 1, 2, 3$. Regardless of whether or not there are within-component gradients, it is evident that mixture distributions (Eqn. 1) do not generally factor into the corresponding marginals - a condition that is necessary for independence. Thus mixtures invariably exhibit some sort of *overall gradient*.

3. Bivariate Scatter Plots and Binning Diagrams

In the study of stellar populations, two types of bivariate diagrams are commonly used to display the data: (1) a scatter plot of the raw data, *i.e.*, y versus x for individual stars or star clusters; and when the sample is sufficiently large, (2) 'binning plots', in which the data are binned according to x and, for each bin, either the mean of the y -values, $\bar{y}(x)$, or the corresponding standard deviation, $s_y(x)$, is plotted against x (the mid-point of the x -values).

Scatter plots, and plots of $\bar{y}(x)$ versus x , which are simply smoothed scatter plots, are useful for depicting overall trends in the relationship between two variables. For example, the A - m scatter plots of Carlberg *et al.* (1985, Fig. 3a) and Schuster & Nissen (1989, Fig. 7), and the $\bar{A}(m)$ - m binning diagrams of Twarog (1980, Figs. 1-3), Carlberg *et al.* (1985, Fig. 3b) and Schuster & Nissen (1989, Table 2), show that, for samples of solar neighbourhood stars, there is a tendency for older stars to be more metal poor. This type of non-linear trend is expected if the data are drawn from a mixture of stellar populations, each of which has a different mean age and mean metal abundance. In fact, if Eqn. 2 holds, the exact functional form of the relationship can be determined by computing the *conditional mean* of A given m (see Paper II).

Patterns of dispersion are often of as much interest as overall trends. For example, a scatter plot of W versus m typically shows no trend in the mean (*i.e.*, the points are scattered about the line $W = 0$) but has an obvious wedge-shaped appearance which is indicative of a heterogeneous variance. Such a pattern can readily be explained by a mixture, in which the constituent stellar populations have different W -dispersions (with $\mu_{Wk} = 0$ for all components k) and different mean metallicities (see Fig. 3 of Paper II). Although scatter plots are useful for identifying heterogeneity in the dispersion, they are not very effective for describing precisely how the dispersion varies. A binning diagram of $s_y(x)$ versus x is more useful for this purpose.

Some examples of this approach are the $s_U(m)$ - m , $s_V(m)$ - m , and $s_W(m)$ - m values, which have been tabulated and plotted by Sandage & Fouts (1987), Carney, Latham & Laird (1989), Yoshii & Saio (1979), and Norris & Ryan (1989). Computation of the *conditional standard deviation* of y given x , under an appropriate mixture model (Eqn. 1 or 2), yields the relevant analytical expression for the dispersion.

The bivariate diagrams described above are generally thought to provide important clues about galactic evolution, such as evidence of a thick-disk component, information about within-component gradients, or features that might suggest the number of components. The great utility of mixture models is that by appealing to theory and to simulations much insight into the interpretation of these diagrams can be gained. For instance, simulated scatter plots of A versus m , and plots of the corresponding conditional mean, can be used to examine the effects of varying the mixing proportions (see Fig.6 of Paper II). Furthermore, if the properties of $s_W(m)$ - m plots are understood (see Fig. 4 of Paper II), then it is clear that such diagrams cannot, in general, be used to determine the number of components in a mixture. They can, however, be useful for examining gradients within components, but only at the extremities of metallicity range where the influence of overlapping components is minimized, if not eliminated. Of course, the exact range over which this is achieved is difficult to determine and there is always the possibility of contamination from unidentified extreme components, *e.g.*, the presence of possible Pop. III stars, or metal-rich bulge stars. Because evidence for a gradient within a given component (*e.g.*, the Norris & Ryan extended disk) always depends on the underlying model (in particular, the assumed number of components - see Fig.3 of Paper II), any conclusions should be accepted with caution. Likewise, claims that one can, using such plots as \bar{V}_{rot} versus m , distinguish between a 'continuum model' and a discrete component mixture model can be misleading, since what is often purported to support the continuum model is often equally explicable by a simple mixture model.

4. Bivariate Posterior Mixing Proportions: Population Membership

The mixing proportion p_k in Eqn. 1 is the unconditional (or overall) probability that a randomly selected star belongs to the k^{th} stellar population. Once age and [Fe/H] measurements have been made, then the probability that the star belongs to a particular population should be revised to take into account this information, *e.g.*, if the star is very metal-poor then the probability that the star belongs to the halo should be adjusted upwards. The revised, or conditional, probabilities are known as *posterior* mixing proportions and will be denoted $p(k|A, m)$, for $k=1,2, 3$. These probabilities are functions of A and m and satisfy the constraint $\sum_{k=1}^K p(k|A, m) = 1$ for each (A, m) .

Posterior mixing proportions are easily calculated using Bayes' Theorem. In the bivariate case of age and metallicity,

$$p(k|A, m) = \frac{p_k f(A, m|k)}{\sum_{j=1}^K p_j f(A, m|j)}. \quad (3)$$

The right-hand side of this equation depends on the unknown model parameters, μ_{Ak} , σ_{Ak} , etc., which must be replaced by estimates before the posterior mixing proportions can be evaluated. Notice that even if A and m are independent for each component, *i.e.*, $f(A, m|k) = f(A|k) f(m|k)$, the posterior probability $p(k|A, m)$ does not factor into the univariate posterior functions.

Fig. 2 shows bivariate posterior mixing proportions $p(k|A, m)$ corresponding to the thick-disk and halo components of the model illustrated in Fig.1. The surfaces give membership probabilities for the thick disk and the halo components, for each value of A and m . In practice,

such diagrams (computed and plotted for any number of components, and based on estimated parameters for a specific catalog of data) provide a quick visual estimate of the probability that a star belongs to a given stellar population.

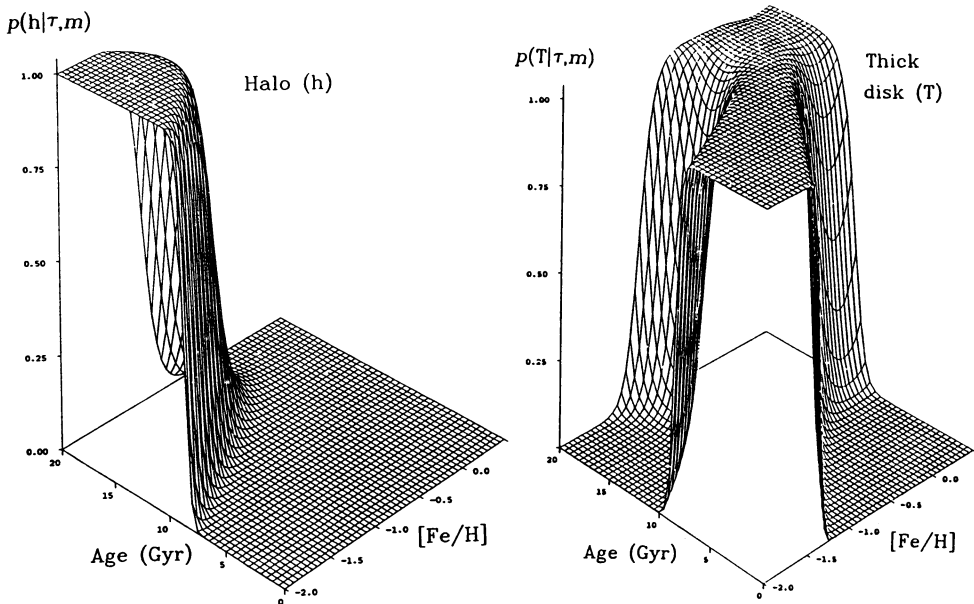


Figure 2. Posterior mixing proportions, conditional on age and metallicity, for the halo and thick-disk components of the three-component Gaussian model shown in Figure 1.

REFERENCES

- Bahcall, J. 1986, *ARA&A* 24, 577.
 Carlberg, R.G., Dawson, P.C., Hsu, T. & Vandenberg, D.A. 1985, *ApJ*, 294, 674.
 Carney, B.W., Latham D.W. & Laird, J.B. 1989, *AJ*, 97, 423.
 Eggen, O.J., Lynden-Bell, D. & Sandage, A.R. 1962, *ApJ*, 136, 748.
 Gilmore, G. & Wyse, R. 1985, *AJ*, 90, 2015.
 Nemeč, J. & Nemeč, A.F.L. 1991a, *PASP*, 103, 95 (Paper I).
 Nemeč, J. & Nemeč, A.F.L. 1991b, *ASP Conf. Ser.*, 13, 512 (Paper II).
 Norris, J. 1986, *ApJS*, 61, 667.
 Norris, J. & Ryan, S. 1989, *ApJ*, 340, 739.
 Sandage, A. 1987a, *AJ*, 93, 610.
 Sandage, A. 1987b, in *The Galaxy*, eds. G.Gilmore & B.Carswell, Dordrecht:Reidel, p.321.
 Sandage, A. & Fouts, G. 1987, *AJ*, 93, 74.
 Schuster, W.J. & Nissen, P.E. 1989, *A&A*, 222, 69.
 Searle, L. & Zinn, R. 1978 *ApJ*, 225, 357.
 Twarog, B. 1980, *ApJ*, 242, 242.
 Yoshii, Y. & Saio, H. 1979, *PASJ*, 31, 339.